环境科学
(HUANJING KEXUE)
ENVIRONMENTAL SCIENCE
第44卷 第7期
2023年7月15日

目 次

加速能源转型与产业结构调整的环境健康协同效益评估:以京津冀鲁地区为例 …… 杨玺,孙奕生,常世彦,李胜悦,郑昊天,王书肖,张希良(3627)
基于不同电力需求的中国减污降碳协同增效路径 …… 向梦宇,王深,吕连宏,张楠,白梓函(3637)
城市碳达峰碳中和行动评估方法与应用 …… 张保留,白梓函,张楠,吕连宏,阳平坚(3649)
基于可解释性机器学习的城市 O_3 驱动因素挖掘 …… 董佳奇,胡冬梅,闫雨龙,彭林,张鹏辉,牛月圆,段小琳(3660)
基于响应曲面法的臭氧生成敏感性分析 …… 朱禹寰,陈冰,张雅铷,刘晓,李光耀,舍静,陈强(3669)
基于 WRF-CMAQ/ISAM 模型的榆林市夏季 O_3 来源解析 …… 王伊凡,仝纪龙,陈羽翔,林鑫,刘永乐,敖丛杰,刘浩天(3676)
基于轻量级梯度提升机的南京大气臭氧浓度预测 …… 朱珈莹,安俊琳,冯悦政,贺婕,张玉欣,王俊秀(3685)
2022年广东省冬季一次臭氧污染过程的气象成因及潜在源区分析 …… 李婷苑,陈靖扬,龚宇,沈劲(3695)
夏季对流层臭氧辐射强迫对华北地区天气和空气质量的影响 …… 杜楠,陈磊,廖宏,朱佳,李柯(3705)
气象、本地光化学生成和外围传输对长沙市2018~2020年臭氧污染趋势变化影响的识别 …… 杨俊,杨雷峰,丁华,谢丹平,刘妍妍,余涛,吕明,袁自冰(3715)
2000~2021年成渝城市群 $PM_{2.5}$ 时空变化及驱动机制多维探测 …… 徐勇,郭振东,郑志威,戴强玉,赵纯,黄雯婷(3724)
基于 GTWR-XGBoost 模型的四川省 $PM_{2.5}$ 小时浓度估算 …… 吴迪,杜宁,王莉,吴宇宏,张少磊,周彬,张显云(3738)
2013~2021年邢台 $PM_{2.5}$ 重污染过程输送和增长特性 …… 江琪,盛黎,靳雨晨,王继康,尤媛,王飞(3749)
基于高分辨率在线观测数据分析上海市城区秋冬季大气有机气溶胶化学特征及污染来源 …… 朱书慧(3760)
机动车尾气碳质气溶胶排放因子及其稳定碳同位素特征 …… 于鸣媛,王谦,付明亮,戈畅,谢锋,曹芳,章炎麟(3771)
沈阳工业区夏季 VOCs 组成特征及其对二次污染形成的贡献 …… 关璐,苏枞枞,库盈盈,胡建林,于兴娜(3779)
疫情管控期间深圳市城区 VOCs 的变化特征及减排效果评估 … 云龙,林楚雄,李成柳,邱志诚,古添发,李光程,张明棣,郭键锋(3788)
西安市冬季道路扬尘中有机质组成特征及其氧化潜势 …… 王擎雯,陈庆彩,王超,王瑞鹤,刘国瑞,李豪,李艳广(3797)
淮北孙疃矿区地表尘中多环芳烃类化合物的污染特征及致癌风险评价 …… 徐振鹏,钱雅慧,洪秀萍,罗钟庚,高秀龙,梁汉东(3809)
雄安建设初期白洋淀水质时空差异及其对降雨和土地利用的响应 …… 王子铭,杨丽虎,宋献方(3820)
流域尺度污染溯源模拟-优化防控方法:以铜陵市顺安河流域为例 …… 刘国王辰,陈磊,李佳奇,张钰晨,赵奕欣,刘妍琪,沈珍瑶(3835)
南昌市浅层地下水水质评价及监测指标优化 …… 郑紫吟,储小东,徐金英,马志飞(3846)
闪电河流域"三水"氢氧同位素特征及水体转换分析 …… 杨丽娜,贾德彬,高瑞忠,苏文旭,卢方园,郝玉胜(3855)
金沙江丰富类和稀有类浮游真核微生物的分布特征与影响因素 …… 燕炳成,崔戈,孙胜浩,王沛芳,王超,吴程,陈娟(3864)
嘉陵江不同干扰断面河道沉积物细菌群落多样性 …… 竹兰萍,张拓,李佳宁,王佳颖,郑伟亮,徐飞,张富斌(3872)
水库水深变化对不同浮游微生物群落及网络互作关键种的影响 …… 王洵,廖琴,王沛芳,袁秋生,胡斌,邢小蕾,徐浩森(3881)
典型工业区地下水细菌群落多样性特征与环境因子响应初探 …… 吴建强,张书源,王敏,陈敏,叶文娟,熊丽君,黄沈发(3892)
太湖流域肥料施用策略调整对典型作物系统氮磷流失的影响 …… 俞映倞,王逸之,杨桹,杨林章,段婧婧,韩雪梅,薛利红(3902)
基于机器学习的长江流域农田氮径流流失负荷估算 …… 张育福,潘哲祺,陈丁江(3913)
千岛湖地区上梧溪流域地表径流非点源氮污染分类识别 …… 俞珂,严琰,唐张轩,张方方,何圣嘉,姜培坤(3923)
沱江和涪江水系干支流氮磷营养盐的空间分布特征 …… 李子阳,周明华,徐鹏,陈露,刘祥龙,林洪羽,江南,任兵,张博文(3933)
外秦淮河底泥污染及疏浚效果 …… 张沐,任增谊,张曼,赵琼,尹洪斌(3945)
新污染物多环芳烃衍生物的来源、分布与光化学行为 …… 葛林科,王子宇,曹胜凯,车晓佳,朱超,张蓬,马宏瑞(3957)
镉砷在针铁矿界面共吸附的相互作用机制 …… 苏子贤,刘赛红,管玉峰,陶亮(3970)
环糊精键合 Fe-TAML 催化剂的制备及其活化 H_2O_2 氧化水中有机微污染物 …… 刘清泉,蔡本哲,蔡喜运(3978)
Co(Ⅱ)活化过一硫酸盐降解氨基三亚甲基膦酸的性能及反应机制 …… 朱敬林,汪舒(3990)
微塑料诱导下污泥造粒潜能变化及微生物富集特征 …… 谢晴帆,俞楠,张妮,谢周云,单珂欣,吴亦馨,唐力,夏静芬,杨国靖(3997)
中国农田土壤 Cd 累积分布特征及概率风险评价 …… 王静,魏恒,潘波(4006)
渝东南典型地质高背景区土壤重金属来源解析及污染评价 …… 蒋玉莲,余京,王锐,王佳彬,李瑜,余飞,张云逸(4017)
基于 PMF 模型的农田土壤重金属源暴露风险综合评价:以浙江省某电子垃圾拆解区为例 …… 方嘉,何影,黄乃涛,支裕优,傅伟军(4027)
乌鲁木齐市郊农田土壤及农作物中多环芳烃的污染特征及风险评价 …… 范悦,曹双瑜,艾力江·努尔拉,于苏云江·吗米提敏,阿不都艾尼·阿不里,谢宣宣,古丽斯坦·阿不都拉,刘河疆(4039)
荒漠绿洲土壤抗生素抗性基因分布特征及驱动机制 …… 黄福义,周曙仡聃,苏建强,朱永官(4052)
近15年我国土壤抗生素污染特征与生物修复研究进展 …… 赵晓东,乔青青,秦宵睿,李晓晶,李永涛(4059)
改性生物炭修复砷镉复合污染土壤研究进展 …… 吕鹏,李莲芳,黄晓雅(4077)
沼液还田对土壤-作物系统重金属累积的影响:Meta 分析 …… 赵奇志,杨志敏,孔凡靖,熊海灵,朱康文,陈玉成(4091)
两种铁改性生物炭对微碱性砷镉污染土壤的修复效果 …… 梁欣冉,何丹,郑罂华,付庆灵,胡红青,朱俊(4100)
秸秆离田对土壤 Cd 生物有效性及水稻 Cd 积累的影响 …… 王子钰,周航,周坤华,谭文韬,蒋毅,唐棋,伍港繁,辜娇峰,曾鹏,廖柏寒(4109)
秸秆与脱硫石膏配施改良黄河三角洲盐碱地的理化性质 …… 赵惠丽,于金艺,刘涛,王丽,赵英(4119)
基于环境 DNA 的复合污染土壤生物评价和胁迫诊断 …… 黄湘云,钟文军,刘训杰,毕婉娟,钱林皓,张效伟(4130)
地质高背景区土壤-玉米重金属综合质量评价 …… 张传华,王钟书,刘力,刘燕(4142)
浙江省蔬菜生产系统重金属污染生态健康风险 …… 张述敏,刘翠玲,杨桂玲,邓美华(4151)
生物炭配施磷肥对土壤养分、酶活性及紫花苜蓿养分吸收的影响 …… 刘鑫裕,王冬梅,张泽洲,张鹏,樊桐桐(4162)
低密度聚乙烯微塑料对空心菜生长和生理特征的影响 …… 周颖,蒋文婷,刘训悦,朱高荻,唐荣贵,章海波,蔡延江(4170)
沼液施用对麦稻茬口期土壤微生物群落结构特征及功能的影响 …… 乔宇颖,奚辉,李娜,陈喜靖,沈阿林,喻曼(4179)
大同铅锌尾矿不同污染程度土壤细菌群落分析及生态功能特征 …… 刘泽勋,庄家尧,刘超,郑康,陈玲(4191)
马尾松采伐迹地火烧黑炭对土壤有机碳组分和碳转化酶活性的影响 …… 姚智,焦鹏宇,吴晓生,严强,刘先,胡亚林,王玉哲(4201)
《环境科学》征订启事(3648)　《环境科学》征稿简则(3659)　信息(3714,4150,4178)

万方知库 Eco-Environmental Knowledge Web

环 境 科 学
Environmental Science

第44卷第7期 2023年7月
Vol.44,No.7 Jul.,2023

基于响应曲面法的臭氧生成敏感性分析

朱禹寰[1],陈冰[2],张雅铷[1],刘晓[1],李光耀[1],佘静[1],陈强[1*]

(1.兰州大学大气科学学院,半干旱气候变化教育部重点实验室,兰州 730000;2.聚光科技(杭州)股份有限公司,杭州 310000)

摘要:准确判断臭氧(O_3)生成敏感性对 O_3 污染成因分析和防控对策的制定至关重要.首次利用响应曲面方法设计最优试验方案,基于盒子模式模拟结果,快速量化 O_3 对其前体物变化的响应.结果表明,CO 对 O_3 有正贡献,NO_x 和 VOCs 与 O_3 呈现显著非线性关系,当 φ(VOCs)与[$\varphi(NO_x)-13.75$]比值大于4.17时,为 NO_x 控制区,小于4.17时,为 VOCs 控制区;烯烃为影响 O_3 生成的关键 VOCs 组分,当 φ(烯烃)与[$\varphi(NO_x)-15$]比值小于1.10且 φ(烯烃)$<35\times10^{-9}$时,烯烃有利于 O_3 的生成.响应曲面法在多因素和其交互作用对 O_3 生成影响的研究中取得了良好效果,为高效判断 O_3 敏感性提供了新的思路和方法.

关键词:臭氧(O_3);响应曲面;O_3 敏感性;盒子模式;一氧化碳(CO);挥发性有机物(VOCs)

中图分类号:X515 **文献标识码**:A **文章编号**:0250-3301(2023)07-3669-07 **DOI**:10.13227/j.hjkx.202208115

Sensitivity Analysis of Ozone Formation Using Response Surface Methodology

ZHU Yu-huan[1], CHEN Bing[2], ZHANG Ya-ru[1], LIU Xiao[1], LI Guang-yao[1], SHE Jing[1], CHEN Qiang[1*]

(1. Key Laboratory for Semi-Arid Climate Change, Ministry of Education, College of Atmospheric Sciences, Lanzhou University, Lanzhou 730000, China; 2. Focused Photonics(Hangzhou) Incorporated Company, Hangzhou 310000, China)

Abstract: Identifying the nonlinear relationship between O_3 and its precursors accurately plays an important role for the policy-making of O_3 pollution control. In this study, the response surface methodology based on the box model simulation was used to quickly and efficiently quantify the O_3 response to their precursors with the optimal experimental design. The results showed that CO had a positive contribution to ozone generation, whereas NO_x and VOCs had a significant nonlinear relationship with O_3. When the ratio of φ(VOCs) to [$\varphi(NO_x)-13.75$] was greater than 4.17, the ozone formation regime was NO_x-limited and became VOCs-limited when the ratio was less than 4.17. Olefin was the key VOCs' component to affect the formation of O_3; when the radio of φ(olefin) to [$\varphi(NO_x)-15$] was less than 1.10 and the value of the φ(olefin) was less than 35×10^{-9}, olefin went far towards generating O_3. Response surface methodology demonstrated that it can be well used to explore the influence of multiple factors and their interactions on O_3 formation and provides a new approach for efficient O_3 sensitivity analysis.

Key words: ozone(O_3); response surface; O_3 sensitivity; box model; carbon monoxide(CO); volatile organic compounds(VOCs)

对流层臭氧(O_3)是环境空气中主要的污染物,对人体健康、植物生长和气候均有不利影响[1~3].O_3 是氮氧化物(NO_x)、挥发性有机化合物(VOCs)和 CO 等前体物发生复杂光化学反应生成的二次污染物[4],其和前体物之间存在高度非线性关系[5],同时颗粒物[6~8]和气象条件[9]等因素通过改变前体物的浓度、物种组成和化学反应速率等也对 O_3 的生成和消耗产生影响.自我国实施《大气污染防治行动计划》等严格大气污染防治政策以来,SO_2、NO_2 和 CO 等污染物浓度明显下降,$PM_{2.5}$ 污染问题得到了较大的改善,但是我国大多数地区 O_3 浓度却呈现波动上升趋势[10~12];2020年初 COVID-19 病毒大流行,疫情管控期间人为活动受到限制使得一次污染物的排放量大幅减少,但在部分地区 O_3 仍保持较高浓度[13],可见对前体物的不当控制可能会导致 O_3 浓度的升高,所以准确判断 O_3 生成对前体物的敏感性是制定有效控制 O_3 污染决策的关键.目前,常见研究 O_3 生成敏感性的方法有 O_3 等值线(O_3 isopleths)、相对增量反应活性(relative incremental reactivity, RIR)和光化学指示剂(photochemical indicator, PI)等[14],其中 PI 阈值的选取受 O_3 污染程度的影响且有较大地区差异[15],所以其应用存在局限性.O_3 等值线是表征 O_3 与前体物之间关系的曲线[16,17],绘制研究区域 O_3 等值线的方法主要分为基于现场观测数据和数值模式模拟两种.基于观测数据的方法是利用反映各因素综合影响的现场观测数据构建 O_3 与 NO_x 和 VOCs 的回归模型[18]、卷积神经网络(CNN)模型[19]或随机森林(RF)模型[20]等得到 O_3 等值线.基于数值模式的方法是利用盒子模式(box models)[21,22]或三维大气化学传输模式(chemical transport models, CTMs)[23~25],模拟 NO_x 和 VOCs 在不同排放或浓度水平下 O_3 的生成,从而绘制等值线.相较于盒子模式来说,多次运行 CTMs 需要非常大的计算资源,高阶解耦直接法(high-order decoupled direct method, HDDM)[26]和响应曲面法(response surface methodolog, RSM)[27~30]等被用于减少 CTMs 的模拟

收稿日期:2022-08-12;**修订日期**:2022-09-30

作者简介:朱禹寰(1997~),女,硕士研究生,主要研究方向为大气污染形成机制,E-mail:zhuyh20@lzu.edu.cn

* 通信作者,E-mail:chenqqh@lzu.edu.cn

次数,以提高构建等值线的效率. 目前在利用 O_3 等值线判断 O_3 生成敏感性的多数研究中,通常考察 NO_x 和 VOCs 两类前体物整体变化的影响[31~33],忽略了不同 VOCs 物种之间的活性差异和其他前体物对 O_3 生成的影响. RIR 被定义为 O_3 生成潜势的变化与前体物浓度变化的比值[34],根据各前体物 RIR 值的正负判断 O_3 生成对其的敏感性[35,36]. RIR 法可以判断具体前体物对 O_3 生成的影响,但其属于单因素分析,未考虑不同 VOCs 物种及和 NO_x 之间交互作用对 O_3 生成的影响.

响应曲面法是通过设计合理的试验方案,利用统计学方法对试验结果进行拟合,构建多因素和其交互作用与响应值间函数关系的方法[37,38],目前在减少 CTMs 模拟次数从而高效绘制 O_3 等值线相关研究中有较为广泛的应用,但尚未发现将其用于探究多因素和其交互作用对 O_3 生成的影响. 针对 O_3 敏感性研究存在的问题,本研究通过利用响应曲面法分析 NO_x、VOCs 和 CO 多因素和其交互作用对 O_3 生成的影响,实现 O_3 对主要前体物生成敏感性的快速判断; 进一步考虑 VOCs 不同物种间活性的差异,探究 NO_x、烷烃、烯烃、芳香烃、醛酮和其交互作用对 O_3 生成的影响,识别 O_3 生成的关键 VOCs 组分并通过·OH收支分析解释其影响显著的原因,以期为判断 O_3 生成敏感性提供新的思路和方法.

1 材料与方法

1.1 模式简介和参数设置

KPP(kinetic preprocessor)是由 Damian 等[39]开发出的模拟大气化学反应动力学过程的软件,是目前空气质量模式的核心模块之一. 采用 KPP-3.0.0 版本,化学机制选用包含 33 个物种和 81 个化学反应的 CBM-Ⅳ[40],输入的初始数据包括 O_3、NO、NO_2、CO 和 VOCs 等污染物以及温度和湿度等,模拟时长为 12 h,分辨率为 60 s.

1.2 模式输入数据来源

选用乌海超级观测站(观测站具体介绍见参考文献[41])某日 10:00 的 NO、NO_2、CO 和 VOCs(包括 29 种烷烃、9 种烯烃、34 种卤代烃、17 种芳香烃、9 种醛类、4 种酮类、3 种醚类、3 种酯类以及异丙醇、二硫化碳和乙炔)监测数据为例,作为基准情景下的污染物组成,各污染物和 VOCs 模式物种的体积分数见表 1 所示.

表 1 基准情景下的污染物组成 $\times 10^{-9}$

Table 1 Initial pollutant composition used in baseline scenario $\times 10^{-9}$

组分	体积分数	组分	体积分数
NO	27.00	CO	1 000.00
NO_2	33.00	VOCs	146.33
PAR	294.78	ETH	17.11
OLE	6.45	TOL	1.62
XYL	2.04	ALD2	5.62

1.3 响应曲面法(RSM)

响应曲面法(RSM)是通过合理的试验设计,采用多元回归方程拟合因素和响应值之间函数关系的统计方法. 中心复合设计(central composite design, CCD)是常用的响应曲面试验设计方法之一,探究 k 个因素对响应值影响的 CCD 方案由中心点、2^k 个顶点和 $2k$ 个定义参数 α 的轴向点组成,其中中心点和顶点用于估计模型的一次项和交互项,轴向点用于估计平方项. 利用 Design-expert 13 软件(试用版),选择 CCD 方法分别设计两组多因素试验情景,即: ①NO_x、VOCs 和 CO; ②NO_x、烷烃、烯烃、芳香烃和醛酮作为影响因素,以 O_3 日最大体积分数(O_{3max})为响应值进行建模.

2 结果与讨论

2.1 NO_x、VOCs 和 CO 这 3 因素对 O_3 生成的影响

利用 CCD 方法设计得到 18 个试验情景(包含 3 个重复试验),探究 NO_x、VOCs 和 CO 对 O_3 生成的影响,试验方案中各因素中心点、顶点和轴向点对应的取值如表 2 所示.

表 2 中心复合设计 3 因素布局水平 $\times 10^{-9}$

Table 2 Level of three-factor layout for CCD $\times 10^{-9}$

因素	中心点取值	顶点取值		轴向点取值	
$A(NO_x)$	60.00	26.40	93.60	0.27	119.73
B(VOCs)	146.00	64.00	228.00	0.22	291.78
C(CO)	1 000.00	440.00	1 560.00	4.44	1 995.56

通过 RSM 建立 $A(NO_x)$、B(VOCs)和 C(CO)与 O_{3max} 的回归方程,如式(1)所示:

$$O_{3max} = -0.74 + 2.21A + 0.36B + 1.3\times10^{-2}C + 8.4\times10^{-3}AB + 2.7\times10^{-5}AC + 3.6\times10^{-5}BC - 0.03A^2 - 1.6\times10^{-3}B^2 - 1.3\times10^{-6}C^2 \quad (1)$$

模型的方差分析结果显示, F 值为 32.30, P 值 $<0.000\,1$,表示模型极显著,具有统计学意义; 调整决定系数 $R^2_{adj} = 0.946\,3$,说明模型能够解释 94.63%

响应值的变化；模型的拟合信噪比为 15.05，大于 4，综上该模型可用于分析前体物 NO_x、VOCs 和 CO 对 O_{3max} 的影响. 根据模型各项的 P 值可得，NO_x 二次项、VOCs 一次项、VOCs 二次项、NO_x 和 VOCs 的交互作用和 CO 一次项均对 O_{3max} 有显著影响，已有研究也表明 NO_x、VOCs 和 CO 均为 O_3 生成的重要前体物[42~45]. 由于 CO 与 NO_x 和 VOCs 的交互作用均不显著，仅 CO 一次项显著且回归方程中 CO 项系数为正，即可得 CO 对 O_{3max} 有正贡献，对 O_3-NO_x-VOCs 敏感性影响较小. 而 NO_x 和 VOCs 存在交互作用且其二次项均显著，说明 O_{3max} 与 NO_x 和 VOCs 存在非线性关系，由回归方程得到 O_3 等值线[图 1(a)]反映 O_3-NO_x-VOCs 敏感性，脊线 $\varphi(NO_x) = 0.24 \times \varphi(VOCs) + 13.75$ 下方区域为 NO_x 控制区，$\varphi(NO_x)$ 增加会导致 O_{3max} 升高，但 φ(VOCs) 对 O_{3max} 影响较小；脊线上方区域为 VOCs 控制区，随着 φ(VOCs) 的增加，O_{3max} 显著升高，$\varphi(NO_x) < 50 \times 10^{-9}$ 时 O_{3max} 对 NO_x 不敏感，但 $\varphi(NO_x) > 50 \times 10^{-9}$ 时 NO_x 存在滴定作用. 图 1(b) 是保持 NO_x 和 VOCs 取值范围相同，对 121 个等浓度梯度情景的模拟结果进行插值得到的 O_3 等值线，其脊线为 $\varphi(NO_x) = 0.28 \times \varphi(VOCs) + 13.75$，两种方法得到的 NO_x 和 VOCs 控制区域面积相差小于 5%，即验证了 RSM 所得结果的可靠性.

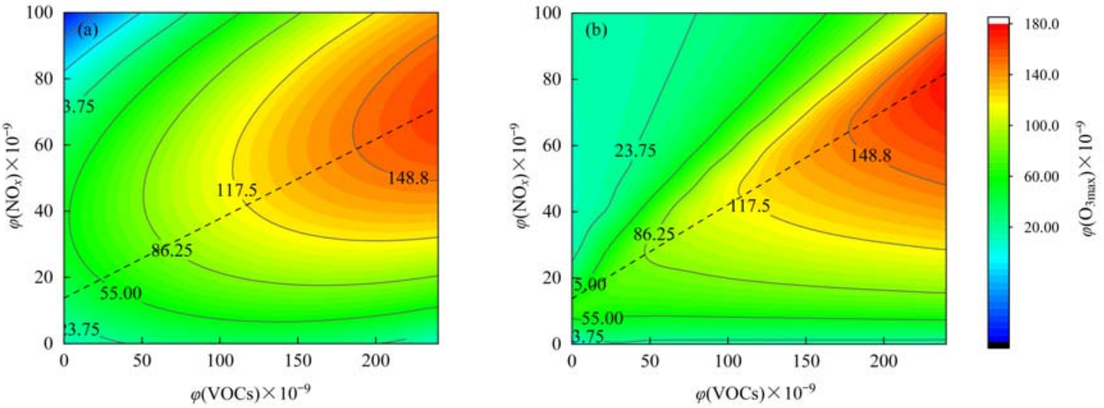

(a) RSM 拟合得到；(b) 121 个 KPP 模拟结果插值得到

图 1　对 NO_x 和 VOCs 变化响应的 O_3 等值线

Fig. 1　Isopleths of the O_3 response to NO_x and VOCs' changes

2.2　NO_x、烷烃、烯烃、芳香烃和醛酮这 5 因素对 O_3 生成的影响

从 2.1 节 3 因素分析结果可得，CO 对 O_{3max} 影响相对较小且其与其他因素间不存在显著交互作用，而 NO_x 和 VOCs 与 O_{3max} 均呈现显著的非线性关系，同时不同 VOCs 反应活性差异较大，因此除了浓度，VOCs 的物种组成对 O_3 生成敏感性也有重要影响. 所以进一步将 VOCs 分为烷烃、烯烃、芳香烃和醛酮，利用 CCD 方法设计得到 46 个试验情景(包含 3 个重复试验)，探究其和 NO_x 对 O_3 生成的影响，试验方案中各因素的中心点、顶点和轴向点对应的取值如表 3 所示.

表 3　中心复合设计 5 因素布局水平 $\times 10^{-9}$

Table 3　Level of five-factor layout for CCD $\times 10^{-9}$

因素	中心点取值	顶点取值		轴向点取值	
$A(NO_x)$	60.00	26.40	93.60	0.27	119.73
B(烷烃)	76.41	33.62	119.20	0.34	152.48
C(烯烃)	23.15	10.18	36.11	0.10	46.19
D(芳香烃)	11.66	5.13	18.19	0.05	23.27
E(醛酮)	35.11	15.45	54.77	0.16	70.06

通过 RSM 建立 $A(NO_x)$、B(烷烃)、C(烯烃)、D(芳香烃)和 E(醛酮)与 O_{3max} 的回归方程如式(2)所示：

$$O_{3max} = 29.84 + 1.94A + 0.10B + 2.27C - 0.25D - 0.12E + 1.8 \times 10^{-3}AB + 0.03AC + 0.02AD + 6.6 \times 10^{-3}AE + 4.5 \times 10^{-3}BC + 1.8 \times 10^{-3}BD + 2.02 \times 10^{-4}BE + 0.03CD + 6.5 \times 10^{-3}CE + 2.4 \times 10^{-3}DE - 0.03A^2 - 1.0 \times 10^{-3}B^2 - 0.07C^2 - 0.05D^2 - 3.6 \times 10^{-3}E^2 \quad (2)$$

模型的方差分析结果显示，F 值为 14.36，$P < 0.0001$ 表示模型极显著，具有统计学意义；调整决定系数 $R^2_{adj} = 0.8586$，说明模型能够解释 85.86% 响应值的变化；模型的拟合信噪比为 14.41，大于 4，

综上该模型可用于分析 NO_x、烷烃、烯烃、芳香烃和醛酮对 O_{3max}的影响. 通过 F 值大小得到各显著项对 O_{3max}影响的排序为: NO_x 二次项 > 烯烃 > NO_x > NO_x 和烯烃的交互作用 > 烯烃二次项 > 烷烃. 在 4 类 VOCs 中, 只有烯烃和烷烃对 O_{3max}有显著影响, 其中烷烃项系数为正, 对 O_3 生成有正贡献; 烯烃一次项和二次项对 O_{3max} 影响都大于烷烃项, 且烯烃与 NO_x 存在交互作用, 综上烯烃可识别为 O_3 生成的关键 VOCs 组分. 图 2 为 NO_x-烯烃-O_3 等值线, 反映 O_{3max}与 NO_x 和烯烃间的非线性关系, 脊线 $\varphi(NO_x) = 0.91 \times \varphi$(烯烃) + 15 下方区域为 NO_x 控制区, NO_x 对 O_{3max}有正贡献, 烯烃对 O_{3max} 影响较小; 脊线上方区域为烯烃控制区, O_{3max}随烯烃的增加而明显升高, 但当 φ(烯烃) > 35×10^{-9}时 O_{3max}呈现略微降低的趋势, 说明高浓度烯烃对 O_3 存在消耗作用, $\varphi(NO_x) < 50 \times 10^{-9}$时 NO_x 对 O_{3max} 影响较小, 但 $\varphi(NO_x) > 50 \times 10^{-9}$时 NO_x 对 O_{3max}存在负贡献.

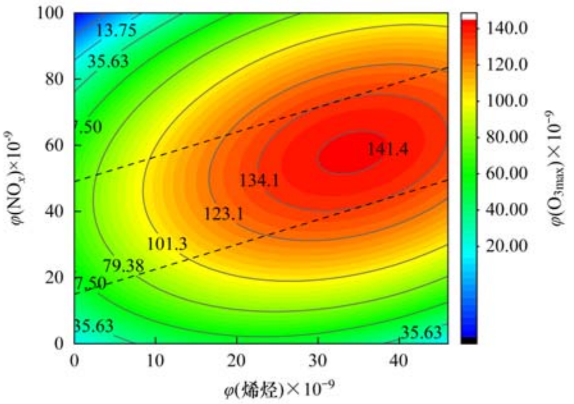

图 2 对 NO_x 和烯烃变化响应的 O_3 等值线

Fig. 2 Isopleth of the O_3 response to NO_x and changes in olefin

为了进一步探究烷烃和烯烃影响 O_3 生成存在较大差异的原因, 对 CCD 方案中 37 ~ 40 号试验情景下(表 4) ·OH的生成和消耗速率进行分析.

表 4 37 ~ 40 号试验情景下各因素值和响应值 $\times 10^{-9}$

Table 4 Value of factors and responses in 37-40 scenario $\times 10^{-9}$

试验情景编号	$A(NO_x)$	B(ALA)	C(OLE)	D(ARO)	E(ALD)	O_{3max}
37	60.00	0.34	23.15	11.66	35.11	107.40
38	60.00	152.48	23.15	11.66	35.11	150.50
39	60.00	76.41	0.10	11.66	35.11	38.56
40	60.00	76.41	46.19	11.66	35.11	159.20

当其他因素均保持中心点值时, 烷烃由轴向点低值[图 3(a)]增加到轴向点高值[图 3(b)], 对应·OH 平均总生成速率由 $(1.1 \pm 0.5) \times 10^7$ molecular·$(cm^3·s)^{-1}$ 升高至 $(1.2 \pm 0.8) \times 10^7$ molecular·$(cm^3·s)^{-1}$, 平均总消耗速率由 $(8.2 \pm 4.7) \times 10^7$ molecular·$(cm^3·s)^{-1}$ 升高至 $(9.5 \pm 6.6) \times 10^7$ molecular·$(cm^3·s)^{-1}$, O_{3max} 升高了 40%; 烯烃由轴向点低值[图 3(c)]增加到轴向点高值[图 3(d)], 对应·OH平均总生成速率由 $(5.2 \pm 2.1) \times 10^6$ molecular·$(cm^3·s)^{-1}$升高至 $(1.5 \pm 1.0) \times 10^7$ molecular·$(cm^3·s)^{-1}$, 平均总消耗速率由 $(3.8 \pm 2.0) \times 10^7$ molecular·$(cm^3·s)^{-1}$升高至 $(1.1 \pm 0.81) \times 10^8$ molecular·$(cm^3·s)^{-1}$, O_{3max} 升高了 313%, 可见烷烃和烯烃增加比例相同时, 烯烃能更有效地促进·OH循环, 从而使 O_{3max} 明显升高.

表 5 为 37 ~ 40 号试验情景下·OH主要生成和消耗途径贡献率, 对比分析各情景下·OH主要生成途径的占比, φ(烯烃)的增加能有效促进 HO_2 将 NO 氧化为 NO_2; 由于 O_3 的光解是 $O(^1D)$的来源, 所以在 O_{3max}较高的情景 38 和 40 中 $O(^1D) + H_2O$ 的贡献较高. 对比各情景下·OH 主要消耗途径的贡献率可得, 相对于烷烃来说, φ(烯烃)的增加更显著地加快了 VOCs + ·OH的反应速率; 同时使 NO_x + ·OH的反应速率降低幅度更大, 烯烃在与 NO_x 争夺·OH时表现出更强的竞争力, 所以其和 NO_x 之间的交互作用对 O_3 生成有重要影响.

表 5 37 ~ 40 号试验情景下, ·OH主要生成和消耗途径贡献率/%

Table 5 Contributions of the main reaction pathways for radical formation and loss in 37-40 scenarios/%

试验情景编号	·OH主要生成途径贡献率			·OH主要消耗途径贡献率			
	HO_2 + NO	$O(^1D) + H_2O$	HONO 光解	VOCs + ·OH	CO + ·OH	NO_2 + ·OH	NO + ·OH
37	62.84	24.33	12.30	40.64	24.81	23.95	8.15
38	58.71	31.17	8.50	58.89	17.99	16.26	4.83
39	50.75	25.57	23.65	34.00	20.36	28.42	15.75
40	55.44	34.36	6.73	61.30	18.81	13.58	3.60

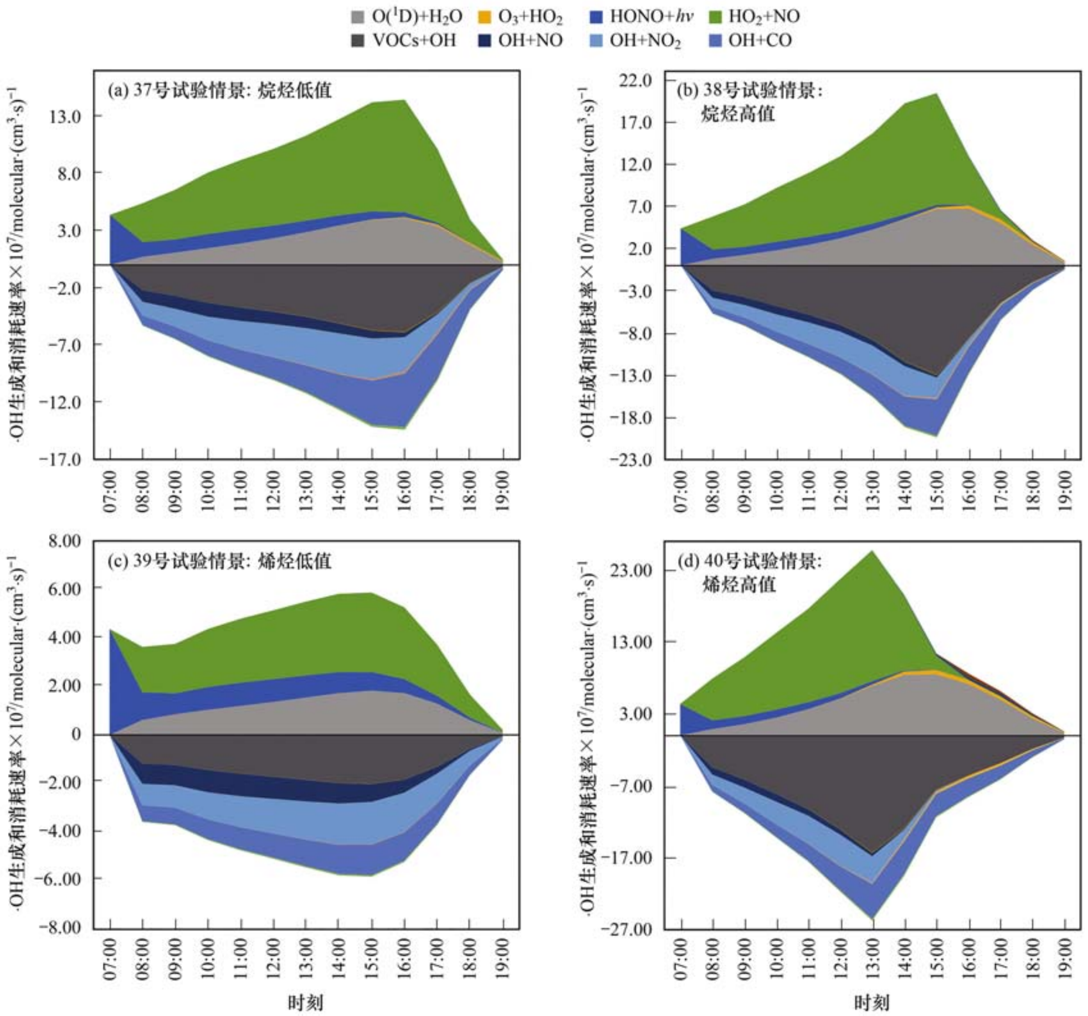

图 3　不同烷烃和烯烃情景下的·OH生成和消耗速率

Fig. 3　Formation and loss rates of ·OH in scenarios with different alkanes and olefins

3　结论

(1)基于结合 CBM-Ⅳ化学机制的盒子模式,设计合理的试验情景,利用响应曲面法建立反映 O_3 和前体物非线性关系的方程,在模拟次数较少的情况下实现多因素和其交互作用对 O_3 生成影响的定量研究,显著提高了 O_3 生成敏感性的判断效率.

(2)CO 对 O_{3max} 有正贡献,其与 NO_x 和 VOCs 的交互作用对 O_{3max} 影响不显著. NO_x 和 VOCs 与 O_{3max} 存在显著非线性关系,当 φ(VOCs)与[$\varphi(NO_x) - 13.75$]比值大于 4.17 时,为 NO_x 控制区;当比值小于 4.17 时,为 VOCs 控制区.

(3)烷烃和烯烃对 O_{3max} 生成影响显著,其中烷烃对 O_{3max} 有正贡献,烯烃和 NO_x 与 O_{3max} 存在显著非线性关系,当 φ(烯烃)与[$\varphi(NO_x) - 15$]比值大于 1.10 时,为 NO_x 控制区;当 φ(烯烃)与[$\varphi(NO_x) - 15$]比值小于 1.10 且 φ(烯烃) $< 35 \times 10^{-9}$ 时,为烯烃控制区,但 φ(烯烃)增加至 35×10^{-9} 以上时,对 O_3 表现出消耗作用.

参考文献:

[1] U.S. EPA. Air quality criteria for ozone and related photochemical oxidants (Final Report, 2006)[R]. EPA/600/R-05/004aF-cF, Washington: U. S. Environmental Protection Agency, 2006.

[2] Turner M C, Jerrett M, Pope Ⅲ C A, *et al*. Long-term ozone exposure and mortality in a large prospective study[J]. American Journal of Respiratory and Critical Care Medicine, 2016, **193**(10): 1134-1142.

[3] Monks P S, Archibald A T, Colette A, *et al*. Tropospheric ozone and its precursors from the urban to the global scale from air quality to short-lived climate forcer[J]. Atmospheric Chemistry and Physics, 2015, **15**(15): 8889-8973.

[4] Haagen-Smit A J. Chemistry and physiology of Los Angeles smog [J]. Industrial & Engineering Chemistry, 1952, **44**(6): 1342-1346.

[5] Sillman S. The relation between ozone, NO_x and hydrocarbons in urban and polluted rural environments [J]. Atmospheric Environment, 1999, **33**(12): 1821-1845.

[6] Chi X Y, Liu C, Xie Z Q, *et al*. Observations of ozone vertical profiles and corresponding precursors in the low troposphere in Beijing, China[J]. Atmospheric Research, 2018, **213**: 224-235.

[7] Li K, Jacob D J, Liao H, *et al*. Anthropogenic drivers of 2013-2017 trends in summer surface ozone in China[J]. Proceedings

of the National Academy of Sciences of the United States of America, 2019, **116**(2): 422-427.
[8] Li K, Jacob D J, Liao H, *et al*. A two-pollutant strategy for improving ozone and particulate air quality in China[J]. Nature Geoscience, 2019, **12**(11): 906-910.
[9] Lu H X, Lyu X, Cheng H R, *et al*. Overview on the spatial-temporal characteristics of the ozone formation regime in China [J]. Environmental Science: Processes & Impacts, 2019, **21**(6): 916-929.
[10] Wang Y H, Gao W K, Wang S, *et al*. Contrasting trends of $PM_{2.5}$ and surface-ozone concentrations in China from 2013 to 2017[J]. National Science Review, 2020, **7**(8): 1331-1339.
[11] Li K, Jacob D J, Shen L, *et al*. Increases in surface ozone pollution in China from 2013 to 2019: anthropogenic and meteorological influences [J]. Atmospheric Chemistry and Physics, 2020, **20**(19): 11423-11433.
[12] Liu Y M, Wang T. Worsening urban ozone pollution in China from 2013 to 2017-Part 1: the complex and varying roles of meteorology[J]. Atmospheric Chemistry and Physics, 2020, **20**(11): 6305-6321.
[13] Cazorla M, Herrera E, Palomeque E, *et al*. What the COVID-19 lockdown revealed about photochemistry and ozone production in Quito, Ecuador[J]. Atmospheric Pollution Research, 2021, **12**(1): 124-133.
[14] Liu C Q, Shi K. A review on methodology in O_3-NO_x-VOC sensitivity study[J]. Environmental Pollution, 2021, **291**, doi: 10.1016/j.envpol.2021.118249.
[15] Liu J W, Li X, Tan Z F, *et al*. Assessing the ratios of formaldehyde and glyoxal to NO_2 as Indicators of O_3-NO_x-VOC sensitivity[J]. Environmental Science & Technology, 2021, **55**(16): 10935-10945.
[16] Chameides W L, Fehsenfeld F, Rodgers M O, *et al*. Ozone precursor relationships in the ambient atmosphere[J]. Journal of Geophysical Research, 1992, **97**(D5): 6037-6055.
[17] Kinosian J R. Ozone-precursor relationships from EKMA diagrams[J]. Environmental Science & Technology, 1982, **16**(12): 880-883.
[18] Qian Y, Henneman L R F, Mulholland J A, *et al*. Empirical development of ozone isopleths: applications to Los Angeles[J]. Environmental Science & Technology Letters, 2019, **6**(5): 294-299.
[19] Santos F M, Gómez-Losada A, Pires J C M. Empirical ozone isopleths at urban and suburban sites through evolutionary procedure-based models [J]. Journal of Hazardous Materials, 2021, **419**, doi: 10.1016/j.jhazmat.2021.126386.
[20] Zhan J L, Liu Y C, Ma W, *et al*. Ozone formation sensitivity study using machine learning coupled with the reactivity of volatile organic compound species[J]. Atmospheric Measurement Techniques, 2022, **15**(5): 1511-1520.
[21] Xie Y T, Cheng C L, Wang Z H, *et al*. Exploration of O_3-precursor relationship and observation-oriented O_3 control strategies in a non-provincial capital city, southwestern China [J]. Science of the Total Environment, 2021, **800**, doi: 10.1016/j.scitotenv.2021.149422.
[22] Hui L R, Ma T, Gao Z J, *et al*. Characteristics and sources of volatile organic compounds during high ozone episodes: a case study at a site in the eastern Guanzhong Plain, China [J]. Chemosphere, 2021, **265**, doi: 10.1016/j.chemosphere.2020.129072.
[23] Luo H H, Zhao K H, Yuan Z B, *et al*. Emission source-based ozone isopleth and isosurface diagrams and their significance in ozone pollution control strategies[J]. Journal of Environmental Sciences, 2021, **105**: 138-149.
[24] Sierra A, Vanoye A Y, Mendoza A. Ozone sensitivity to its precursor emissions in northeastern Mexico for a summer air pollution episode[J]. Journal of the Air & Waste Management Association, 2013, **63**(10): 1221-1233.
[25] Cui M, An X Q, Xing L, *et al*. Simulated sensitivity of ozone generation to precursors in Beijing during a high O_3 episode[J]. Advances in Atmospheric Sciences, 2021, **38**(7): 1223-1237.
[26] Shen H Z, Sun Z, Chen Y L, *et al*. Novel method for ozone isopleth construction and diagnosis for the ozone control strategy of Chinese cities [J]. Environmental Science & Technology, 2021, **55**(23): 15625-15636.
[27] Xing J, Wang S X, Jang C, *et al*. Nonlinear response of ozone to precursor emission changes in China: a modeling study using response surface methodology [J]. Atmospheric Chemistry and Physics, 2011, **11**(10): 5027-5044.
[28] Xing J, Ding D, Wang S X, *et al*. Quantification of the enhanced effectiveness of NO_x control from simultaneous reductions of VOC and NH_3 for reducing air pollution in the Beijing-Tianjin-Hebei region, China[J]. Atmospheric Chemistry and Physics, 2018, **18**(11): 7799-7814.
[29] Xing J, Zheng S X, Ding D, *et al*. Deep learning for prediction of the air quality response to emission changes [J]. Environmental Science & Technology, 2020, **54**(14): 8589-8600.
[30] Li J Y, Dai Y Z, Zhu Y, *et al*. Improvements of response surface modeling with self-adaptive machine learning method for $PM_{2.5}$ and O_3 predictions[J]. Journal of Environmental Management, 2022, **303**, doi: 10.1016/j.jenvman.2021.114210.
[31] 钱骏, 徐晨曦, 陈军辉, 等. 2020年成都市典型臭氧污染过程特征及敏感性[J]. 环境科学, 2021, **42**(12): 5736-5746.
Qian J, Xu C X, Chen J H, *et al*. Chemical characteristics and contaminant sensitivity during the typical ozone pollution processes of Chengdu in 2020 [J]. Environmental Science, 2021, **42**(12): 5736-5746.
[32] 李凯, 刘敏, 梅如波. 泰安市大气臭氧污染特征及敏感性分析[J]. 环境科学, 2020, **41**(8): 3539-3546.
Li K, Liu M, Mei R B. Pollution characteristics and sensitivity analysis of atmospheric ozone in Taian City[J]. Environmental Science, 2020, **41**(8): 3539-3546.
[33] Liu Y F, Qiu P P, Li C L, *et al*. Evolution and variations of atmospheric VOCs and O_3 photochemistry during a summer O_3 event in a county-level city, Southern China[J]. Atmospheric Environment, 2022, **272**, doi: 10.1016/j.atmosenv.2022.118942.
[34] Cardelino C A, Chameides W L. An observation-based model for analyzing ozone precursor relationships in the urban atmosphere [J]. Journal of the Air & Waste Management Association, 1995, **45**(3): 161-180.
[35] Xue L K, Wang T, Gao J, *et al*. Ground-level ozone in four Chinese cities: precursors, regional transport and heterogeneous processes[J]. Atmospheric Chemistry and Physics, 2014, **14**(23): 13175-13188.
[36] An J L, Zou J N, Wang J X, *et al*. Differences in ozone photochemical characteristics between the megacity Nanjing and its suburban surroundings, Yangtze River Delta, China [J]. Environmental Science and Pollution Research, 2015, **22**(24): 19607-19617.
[37] Box G E P, Wilson K B. On the experimental attainment of optimum conditions[J]. Journal of the Royal Statistical Society:

Series B (Methodological), 1951, **13**(1): 1-38.

[38] 刘祥, 王婧瑶, 吴娟娟, 等. 微藻固定化条件优化及其污水氨氮去除潜力分析[J]. 环境科学, 2019, **40**(7): 3126-3134.
Liu X, Wang J Y, Wu J J, *et al*. Optimization of the parameters for microalgae immobilization and analysis of its recovery potential for ammonia nitrogen in wastewater[J]. Environmental Science, 2019, **40**(7): 3126-3134.

[39] Damian V, Sandu A, Damian M, *et al*. The kinetic preprocessor KPP-a software environment for solving chemical kinetics[J]. Computers & Chemical Engineering, 2002, **26**(11): 1567-1579.

[40] Gery M W, Whitten G Z, Killus J P, *et al*. A photochemical kinetics mechanism for urban and regional scale computer modeling[J]. Journal of Geophysical Research, 1989, **94**(D10): 12925-12956.

[41] 朱玉凡, 陈强, 刘晓, 等. 基于气团老化程度对挥发性有机物分类改善 PMF 源解析效果[J]. 环境科学, 2022, **43**(2): 707-713.
Zhu Y F, Chen Q, Liu X, *et al*. Improved performance of PMF source apportionment for volatile organic compounds based on classification of VOCs' aging degree in air mass[J]. Environmental Science, 2022, **43**(2): 707-713.

[42] Wang T, Xue L K, Brimblecombe P, *et al*. Ozone pollution in China: a review of concentrations, meteorological influences, chemical precursors, and effects[J]. Science of the Total Environment, 2017, **575**: 1582-1596.

[43] Atkinson R. Atmospheric chemistry of VOCs and NO_x[J]. Atmospheric Environment, 2000, **34**(12-14): 2063-2101.

[44] Sillman S, Logan J A, Wofsy S C. The sensitivity of ozone to nitrogen oxides and hydrocarbons in regional ozone episodes[J]. Journal of Geophysical Research, 1990, **95**(D2): 1837-1851.

[45] Christian K E, Brune W H, Mao J Q, *et al*. Global sensitivity analysis of GEOS-Chem modeled ozone and hydrogen oxides during the INTEX campaigns[J]. Atmospheric Chemistry and Physics, 2018, **18**(4): 2443-2460.

HUANJING KEXUE

Environmental Science (monthly)

Vol. 44 No. 7

Jul. 15, 2023

CONTENTS

Assessing the Environmental and Health Co-benefits of Accelerated Energy Transition and Industrial Restructuring: A Case Study of the BTHS Region ······ YANG Xi, SUN Yi-sheng, CHANG Shi-yan, *et al.* (3627)
Synergistic Paths of Reduced Pollution and Carbon Emissions Based on Different Power Demands in China ······ XIANG Meng-yu, WANG Shen, LÜ Lian-hong, *et al.* (3637)
Evaluation Method and Application for Urban Carbon Peaking & Neutrality Performance ······ ZHANG Bao-liu, BAI Zi-han, ZHANG Nan, *et al.* (3649)
Revealing Driving Factors of Urban O_3 Based on Explainable Machine Learning ······ DONG Jia-qi, HU Dong-mei, YAN Yu-long, *et al.* (3660)
Sensitivity Analysis of Ozone Formation Using Response Surface Methodology ······ ZHU Yu-huan, CHEN Bing, ZHANG Ya-ru, *et al.* (3669)
Analysis of O_3 Sources in Yulin City in Summer Based on WRF-CMAQ/ISAM Model ······ WANG Yi-fan, TONG Ji-long, CHEN Yu-xiang, *et al.* (3676)
Atmospheric Ozone Concentration Prediction in Nanjing Based on LightGBM ······ ZHU Jia-ying, AN Jun-lin, FENG Yue-zheng, *et al.* (3685)
Meteorological Formation Mechanisms and Potential Sources of an Ozone Pollution Process in Winter of 2022 in Guangdong Province ······ LI Ting-yuan, CHEN Jing-yang, GONG Yu, *et al.* (3695)
Impact of Summer Tropospheric Ozone Radiative Forcing on Meteorology and Air Quality in North China ······ DU Nan, CHEN Lei, LIAO Hong, *et al.* (3705)
Identification of Impacts from Meteorology and Local and Transported Photochemical Generation on Ozone Trends in Changsha from 2018 to 2020 ······ YANG Jun, YANG Lei-feng, DING Hua, *et al.* (3715)
Spatio-temporal Variation and Multi-dimensional Detection of Driving Mechanism of $PM_{2.5}$ Concentration in the Chengdu-Chongqing Urban Agglomeration from 2000 to 2021 ······ XU Yong, GUO Zhen-dong, ZHENG Zhi-wei, *et al.* (3724)
Estimation of $PM_{2.5}$ Hourly Concentration in Sichuan Province Based on GTWR-XGBoost Model ······ WU Di, DU Ning, WANG Li, *et al.* (3738)
Transmission and Growth Characteristics of Severe $PM_{2.5}$ Pollution Events from 2013 to 2021 in Xingtai, Hebei ······ JIANG Qi, SHENG Li, JIN Yu-chen, *et al.* (3749)
Chemical Characteristics and Source Apportionment of Organic Aerosols in Urban Shanghai During Cold Season Based on High Time-resolution Measurements of Organic Molecular Markers ······ ZHU Shu-hui (3760)
Emission Factors of Carbonaceous Aerosol and Stable Carbon Isotope for In-use Vehicles ······ YU Ming-yuan, WANG Qian, FU Ming-liang, *et al.* (3771)
Composition Characteristics of Volatile Organic Compounds and Associated Contributions to Secondary Pollution in Shenyang Industrial Area in Summer ······ GUAN Lu, SU Cong-cong, KU Ying-ying, *et al.* (3779)
Characteristics of VOCs and Assessment of Emission Reduction Effect During the Epidemic Lockdown Period in Shenzhen Urban Area ······ YUN Long, LIN Chu-xiong, LI Cheng-liu, *et al.* (3788)
Characteristics of Organic Matter Composition and Oxidation Potential in Road Dust in Winter in Xi'an ······ WANG Qing-wen, CHEN Qing-cai, WANG Chao, *et al.* (3797)
Contamination Characteristics and Risk Assessment of Polycyclic Aromatic Compounds in Surface Dust of Suntuan Mining Area in Huaibei ······ XU Zhen-peng, QIAN Ya-hui, HONG Xiu-ping, *et al.* (3809)
Spatial-temporal Variation in Water Quality and Its Response to Precipitation and Land Use in Baiyangdian Lake in the Early Stage of the Construction of Xiong'an New Area ······ WANG Zi-ming, YANG Li-hu, SONG Xian-fang (3820)
Simulation of Pollution Apportionment and Optimization of Control Methods in Watershed Scale: A Case Study of the Shun'an Watershed in Tongling City ······ LIU Guo-wangchen, CHEN Lei, LI Jia-qi, *et al.* (3835)
Evaluation of Shallow Groundwater Quality and Optimization of Monitoring Indicators in Nanchang ······ ZHENG Zi-yin, CHU Xiao-dong, XU Jin-ying, *et al.* (3846)
Hydrogen and Oxygen Isotopic Characteristics and Influencing Factors of "Three Waters" in Shandian River Basin ······ YANG Li-na, JIA De-bin, GAO Rui-zhong, *et al.* (3855)
Distribution Characteristics and Influencing Factors of Abundant and Rare Planktonic Microeukaryotes in Jinsha River ······ YAN Bing-cheng, CUI Ge, SUN Sheng-hao, *et al.* (3864)
Bacterial Community Diversity in Channel Sediments of Different Disturbance Sections of the Jialing River ······ ZHU Lan-ping, ZHANG Tuo, LI Jia-ning, *et al.* (3872)
Effects of Reservoir Water Depth on Different Plankton Communities and Keystone Species of Network Interaction ······ WANG Xun, LIAO Qin, WANG Pei-fang, *et al.* (3881)
Correlation Between the Diversity Characteristics of Groundwater Bacterial Community and Environmental Factors in Typical Industrial Areas ······ WU Jian-qiang, ZHANG Shu-yuan, WANG Min, *et al.* (3892)
Effects of Fertilizer Application Strategy Adjustments on Nitrogen and Phosphorus Loss from Typical Crop Systems in Taihu Lake Region ······ YU Ying-liang, WANG Yi-zhi, YANG Bei, *et al.* (3902)
Estimation of Cropland Nitrogen Runoff Loss Loads in the Yangtze River Basin Based on the Machine Learning Approaches ······ ZHANG Yu-fu, PAN Zhe-qi, CHEN Ding-jiang (3913)
Classification and Identification of Non-point Source Nitrogen Pollution in Surface Flow of the Shangwu River Watershed in the Qiandao Lake Region ······ YU Ke, YAN Yan, TANG Zhang-xuan, *et al.* (3923)
Spatial Distribution of Nitrogen and Phosphorus Nutrients in the Main Stream and Typical Tributaries of Tuojiang River and Fujiang River ······ LI Zi-yang, ZHOU Ming-hua, XU Peng, *et al.* (3933)
Sediment Pollution and Dredging Effect of Waiqinhuai River ······ ZHANG Mu, REN Zeng-yi, ZHANG Man, *et al.* (3945)
Critical Review on Environmental Occurrence and Photochemical Behavior of Substituted Polycyclic Aromatic Hydrocarbons ······ GE Lin-ke, WANG Zi-yu, CAO Sheng-kai, *et al.* (3957)
Cadmium and Arsenic Interactions During Co-adsorption onto Goethite ······ SU Zi-xian, LIU Sai-hong, GUAN Yu-feng, *et al.* (3970)
Preparation of Catalyst Cyclodextrin-Fe-TAML to Activate H_2O_2 and Oxidize Organic Micropollutants in Water ······ LIU Qing-quan, CAI Ben-zhe, CAI Xi-yun (3978)
Performance and Reaction Mechanism of Co(Ⅱ) Mediated Activation of Peroxymonosulfate for Degrading Nitrilotris (Methylene Phosphonic Acid) ······ ZHU Jing-lin, WANG Shu (3990)
Change in Granulation Potential and Microbial Enrichment Characteristics of Sludge Induced by Microplastics ······ XIE Qing-fan, YU Nan, ZHANG Ni, *et al.* (3997)
Accumulation Characteristics and Probabilistic Risk Assessment of Cd in Agricultural Soils Across China ······ WANG Jing, WEI Heng, PAN Bo (4006)
Source Analysis and Pollution Assessment of Soil Heavy Metals in Typical Geological High Background Area in Southeastern Chongqing ······ JIANG Yu-lian, YU Jing, WANG Rui, *et al.* (4017)
Integrated Analysis on Source-exposure Risk of Heavy Metals in Farmland Soil Based on PMF Model: A Case Study in the E-waste Dismantling Area in Zhejiang Province ······ FANG Jia, HE Ying, HUANG Nai-tao, *et al.* (4027)
Pollution Characteristics and Risk Assessment of Polycyclic Aromatic Hydrocarbons in Farmland Soil and Crops in the Suburbs of Urumqi ······ FAN Yue, CAO Shuang-yu, Nuerla Ailijiang, *et al.* (4039)
Distribution and Driving Mechanisms of Antibiotic Resistance Genes in Desert-Oasis Continuum ······ HUANG Fu-yi, ZHOU Shu-yidan, SU Jian-qiang, *et al.* (4052)
Characteristics of Antibiotic Contamination of Soil in China in Past Fifteen Years and the Bioremediation Technology: A Review ······ ZHAO Xiao-dong, QIAO Qing-qing, QIN Xiao-rui, *et al.* (4059)
Modified Biochar for Remediation of Soil Contaminated with Arsenic and Cadmium: A Review ······ LÜ Peng, LI Lian-fang, HUANG Xiao-ya (4077)
Effect of Biogas Slurry Return to Field on Heavy Metal Accumulation in Soil-crop System: A Meta-analysis ······ ZHAO Qi-zhi, YANG Zhi-min, KONG Fan-jing, *et al.* (4091)
Remediation Effect of Two Iron-modified Biochars on Slightly Alkaline Arsenic and Cadmium Contaminated Soil ······ LIANG Xin-ran, HE Dan, ZHENG Zhao-hua, *et al.* (4100)
Effects of Straw Removal Measure on Soil Cd Bioavailability and Rice Cd Accumulation ······ WANG Zi-yu, ZHOU Hang, ZHOU Kun-hua, *et al.* (4109)
Application of Desulphurized Gypsum with Straw to Improve Physicochemical Properties of Saline-alkali Land in Yellow River Delta ······ ZHAO Hui-li, YU Jin-yi, LIU Tao, *et al.* (4119)
Biological Evaluation and Key Stress Factor Diagnosis of Compound Contaminated Soil Based on Environmental DNA ······ HUANG Xiang-yun, ZHONG Wen-jun, LIU Xun-jie, *et al.* (4130)
Comprehensive Quality Assessment of Soil-Maize Heavy Metals in High Geological Background Area ······ ZHANG Chuan-hua, WANG Zhong-shu, LIU Li, *et al.* (4142)
Ecological Risk and Health Risk of Heavy Metal Pollution in Vegetable Production System of Zhejiang Province ······ ZHANG Shu-min, LIU Cui-ling, YANG Gui-ling, *et al.* (4151)
Effect of Biochar with Phosphorus Fertilizer on Soil Nutrients, Enzyme Activity, and Nutrient Uptake of *Alfalfa* ······ LIU Xin-yu, WANG Dong-mei, ZHANG Ze-zhou, *et al.* (4162)
Effects of Low-density Polyethylene Microplastics on the Growth and Physiology Characteristics of *Ipomoea aquatica* Forsk ······ ZHOU Ying, JIANG Wen-ting, LIU Xun-yue, *et al.* (4170)
Effects of Biogas Slurry Application on Soil Microbial Communities Structure and Function During Wheat-rice Stubble Period ······ QIAO Yu-ying, XI Hui, LI Na, *et al.* (4179)
Analysis of Soil Bacterial Community Structure and Ecological Function Characteristics in Different Pollution Levels of Lead-zinc Tailings in Datong ······ LIU Ze-xun, ZHUANG Jia-yao, LIU Chao, *et al.* (4191)
Effect of Fire-deposited Charcoal on Soil Organic Carbon Pools and Associated Enzyme Activities in a Recently Harvested *Pinus massoniana* Plantation Subjected to Broadcast Burning ······ YAO Zhi, JIAO Peng-yu, WU Xiao-sheng, *et al.* (4201)